Computing equation of state parameters of gases from Monte Carlo simulations

Ramdin, Mahinder; Becker, Tim M.; Jamali, Seyed Hossein; Wang, M.; Vlugt, Thijs J H

DOI
10.1016/j.fluid.2016.06.012

Publication date
2016

Document Version
Accepted author manuscript

Published in
Fluid Phase Equilibria

Computing equation of state parameters of gases from Monte Carlo simulations

Mahinder Ramdin, Tim M. Becker, Seyed Hossein Jamali, Meng Wang, Thijs J.H. Vlugt*

Engineering Thermodynamics, Process & Energy Department, Faculty of Mechanical, Maritime and Materials Engineering, Delft University of Technology, Leeghwaterstraat 39, 2628CB Delft, The Netherlands

Abstract

Monte Carlo (MC) simulations in ensembles with a fixed chemical potential or fugacity, for example the grand-canonical or the osmotic ensemble, are often used to compute phase equilibria. Chemical potentials can be computed either with an equation of state (EoS) or from molecular simulations. The accuracy of the computed chemical potentials depends on the quality of the (critical) parameters used in the EoS and the applied force field in the simulations. We investigated the consistency of both approaches for computing fugacities of the industrially relevant gases CO_2, CH_4, CO, H_2, N_2, and H_2S. The critical temperature (T_c), pressure (P_c), and acentric factors (ω) of these gases are computed from MC simulations in the Gibbs ensemble. The effect of cutoff radius and tail corrections on the computed values of T_c, P_c, and ω is investigated. In addition, MC simulations in the Gibbs ensemble are used to compute the VLE of the 15 possible binary systems comprising the gases CO_2, CH_4, CO, H_2, N_2, and H_2S, and the ternary systems $CO_2/CH_4/H_2S$ and $CO_2/CO/H_2$. Binary interaction parameters (k_{ij}) of these natural/synthesis gas mixtures are obtained by fitting the Peng-Robinson (PR) EoS to the binary VLE data from the MC simulations. The computed properties from the MC simulations are compared with the PR EoS, the GERG EoS, and experimental results. The MC results show that including tail corrections in the simulations is crucial to obtain accurate critical properties. The force fields used for the gases can reproduce the fugacities of the gases within 5% of

*Corresponding author

Email address: t.j.h.vlugt@tudelft.nl (Thijs J.H. Vlugt)

the experimental data. The dew-point curves of all the 15 binaries were predicted correctly by the MC simulations, but the bubble-point curves for the systems H_2/CO, CH_4/H_2, H_2S/N_2, and H_2S/CO significantly deviate from the experiments.

Keywords: Molecular Simulation, Equation of State, Natural Gas, Synthesis Gas, Binary Interaction Parameter

1. Introduction

Phase equilibria calculations are extremely important for designing and operating industrial processes [1–3]. Equation of states (EoSs) are widely used for this purpose, but often accurate experimental data is required to calibrate the EoS parameters [3]. Alternatively, molecular simulations can be used to compute phase equilibria from the knowledge of molecular properties [4–6]. Different types of ensembles (e.g., Gibbs, grand-canonical, osmotic, etc.) have been devised to perform phase equilibrium calculations using MC simulations [7, 8]. The grand-canonical (μVT) ensemble is mostly used to compute adsorption properties, while the Gibbs or osmotic ensemble is prefered for absorption studies [9–20]. In ensembles with a fixed chemical potential or fugacity (e.g., μVT and osmotic ensemble), the gas phase is often described by an equation of state, while the properties of the adsorbed/absorbed phase are computed from the simulations [21, 22]. Note that any suitable EoS can be used to describe the gas phase, but due to its simplicity and effectiveness, the Peng-Robinson (PR) EoS is often used in MC simulations as well as in industry [23–27]. In principal, it is possible to compute the gas phase chemical potentials from molecular simulations, but the use of an EoS considerably reduces the simulation time. However, it remains questionable whether or not the computed chemical potentials from the EoS are consistent with the molecular models used for the gases. The Lennard-Jones (LJ) parameters of the molecules are typically fitted to experimental pure component vapor-luiquid equilibrium (VLE) data, vapor pressures, and sometimes to binary VLE data [28, 29]. Therefore, it is often assumed that these molecular models or force fields can reproduce fugacities that are consistent with the PR EoS and experiments. Note that the PC-SAFT EoS does not require critical properties of the components, but it also contains a binary interaction parameter, which is fitted to VLE data [30].

This a priori assumption is tested by computing the critical temperatures

(T_c), critical presssures (P_c), acentric factors (ω), densities (ρ), and fugacities (f) of the gases CO_2, CH_4, CO, H_2, N_2, and H_2S using MC simulations in the Gibbs ensemble (GEMC) and the NPT ensemble. The effect of the cutoff radius and the use of tail corrections on these properties is investigated. Additionally, MC simulations in the Gibbs ensemble have been used to compute binary and ternary phase diagrams of natural/synthesis gas mixtures. Subsequently, the properties computed from the MC simulations are compared with the PR EoS [31], the GERG EoS [32], and experimental results.

2. Simulation Details

The TraPPE (united-atom) force field has been used for the gases CO_2, CH_4, N_2 and H_2S [28, 33]. The model of Martín-Calvo et al. [34] has been used for CO and the two-center Lennard-Jones model of Cracknell has been used for H_2 [34, 35]. All the gas molecules were treated as rigid in the MC simulations. The Lorentz-Berthelot combining rules were used for the LJ interactions between dissimilar atoms [5]. The Ewald method was used with a relative precision of 10^{-5} to account for the electrostatic interactions [22, 36]. Three sets of simulations were performed to investigate the effect of the cutoff radius and tail corrections on the computed properties. In the first set, the LJ interactions were truncated and shifted at 12 Å and no tail corrections were applied. In the second set, the LJ interaction were truncated and shifted at 14 Å and tail corrections were excluded. In the third set, the LJ interactions for the TraPPE molecules were truncated at 14 Å and analytical tail corrections [4, 5] were applied conform the TraPPE methodology. In accordance with the Gibbs phase-rule, the VLE of the unary systems were computed form MC simulations in the NVT-Gibbs ensemble. The VLE of the binary and ternary gas mixtures were computed from MC simulations in the NPT-Gibbs ensemble. Note that there is no fundamental objection to use the NVT-Gibbs ensemble to compute VLE of binary, ternary or multicomponent systems. However, the NPT-Gibbs ensemble is more practical for these systems, since it allows a direct comparison with experiments, which are typically performed at constant T and P [37]. In the Gibbs ensemble, two simulation boxes are used to compute properties of coexisting phases. The thermodynamic conditions for phase coexistence unequivocally require that each region is in internal equilibrium, and that the temperature, pressure, and chemical potentials of all components are equal in coexisting regions. In order to satisfy these equilibrium conditions, four kinds of MC moves

(i.e., translation, rotation, volume change, and molecule transfer) are performed in the Gibbs ensemble [4, 8]. The temperature in MC simulations is fixed, while particles are displaced and rotated within each box to satisfy the condition of internal equilibrium, the volume of each box is allowed to fluctuate to equalize the pressure, and particles are transfered between the boxes to satisfy equality of chemical potentials of all components throughout the phases [8]. The densities and fugacities of the gases were computed from MC simulations in the NPT ensemble. The number of molecules in the GEMC simulations and the NPT simulations were computed based on experimental (coexistence) density data. The simulation conditions were chosen based on the availability of experimental data and away from the critical points of the pure components and/or the mixtures. In a Gibbs ensemble simulation, no VLE can be observed close to critical points, because the simulation boxes switch identity (i.e., the box containing the gas might switch and keep switching during the course of the simulation with the box containing the liquid and vice versa) [38]. The histogram reweighting method has the potential to be more accurate, especially near-critical points, but the GEMC simulations are more straightforward to perform and yields accurate critical properties even for relatively small system sizes [38]. Note that the number of particles in the Gibbs ensemble simulations should be initially distributed such that (1) both boxes remain larger than twice the cutoff radius and (2) the initial mole fraction $(N_{i,a} + N_{j,a})/(N_{1,t} + N_{2,t})$ of component a, where subscripts i and j denote the boxes, and t the total number of particles in box i and j, is between x_a and y_a, which are the (experimental) equilibrium composition of component a in the liquid and gas phase, respectively. Failling to satisfy condition (2) will lead to a very long simulation time before a steady state phase split is observed. Condition (1) requires the density of both phases at given T, P, and composition, which can readily be computed from an equation of state (e.g., the PR EoS). All the MC simulations were performed using the molecular simulation tool RASPA [21, 22]. The GEMC and the NPT simulations were started with an equilibration run of 50000 MC cycles, where the number of MC steps in a cycle equals the total number of molecules in the simulation box. In this equilibration run, maximum particle displacements, rotation angles, and maximum volume changes were adjusted such that on average 50 % of the trial moves were accepted. The production runs of the GEMC simulations and the NPT simulations typically consisted of 0.5 million MC cycles.

3. Results and Discussion

MC simulations have been used to compute the parameters of the Peng-Robinson (PR) equation of state (EoS) for the gases CO_2, CH_4, CO, H_2, N_2, and H_2S. The PR EoS is applicable to pure components as well as for mixtures and is given by [31],

$$P = \frac{RT}{v-b} - \frac{a}{v(v+b)+b(v-b)} \tag{1}$$

where v is the molar volume, a and b the pure component parameters accounting for the molecular interaction and co-volume, respectively. For mixtures, the pure component constants, a and b, can be replaced by the parameters of the mixture (a_m and b_m) using the quadratic van der Waals (vdW) mixing rules [3],

$$a_m = \sum_i \sum_j x_i x_j a_{ij}, \qquad a_{ij} = \sqrt{a_i a_j}(1-k_{ij}), \qquad k_{ii} = k_{jj} = 0 \tag{2}$$

$$b_m = \sum_i \sum_j x_i x_j b_{ij}, \qquad b_{ij} = \frac{1}{2}(b_i + b_j)(1-l_{ij}), \qquad l_{ii} = l_{jj} = 0 \tag{3}$$

where k_{ij} and l_{ij} represent the binary interaction parameters. For gas mixtures, only the k_{ij} is used and the l_{ij}, which is typically required for strongly associating systems is set to zero [39, 40]. The computation of a and b requires the critical temperature, critical pressure, and the acentric factor of the components. In the following, we show how these parameters can be obtained from MC simulations.

3.1. Critical parameters and acentric factors

The critical temperature (T_c) and density (ρ_c) are obtained by fitting the subcritical saturated density, ρ_{liq} and ρ_{vap}, data from the GEMC simulations to the law of rectilinear diameters and the scaling law for the density [4],

$$\frac{\rho_{\text{liq}} + \rho_{\text{vap}}}{2} = \rho_c + A(T - T_c) \tag{4}$$

$$\rho_{\text{liq}} - \rho_{\text{vap}} = B|T - T_c|^{\beta} \tag{5}$$

where the critical exponent of a 3-dimensional Ising fluid, $\beta = 0.326$ [38], is used.

The critical pressure, P_c, is obtained from a Clausius-Clapeyron plot by extrapolating the saturated vapor pressure (P^{sat}) data obtained from the GEMC simulations to the critical temperature. The integrated form of the Clausius-Clapeyron equation is given by [2],

$$\ln \frac{P}{P_0} = \frac{-\Delta H_{\text{vap}}}{RT} + C \tag{6}$$

where ΔH_{vap} is the vaporization enthalpy, which can be obtained from the slope of a $\ln P^{\text{sat}}$ vs. $1/T$ plot. An estimate of the critical pressure is obtained by substituting the critical temperature in Equation (6). Unfortunately, the critical pressure obtained in this way will not be consistent with the PR EoS. The reason for this is that the critical compressibility factor of the PR EoS, obtained by imposing the critical contstraints, is a constant [2]:

$$Z_c = \frac{P_c V_c}{RT_c} = 0.307 \tag{7}$$

Consequently, once the critical molar volume ($V_c = M_w/\rho_c$, where M_w is the molecular weight) and T_c are known (i.e., computed from Equations (4) and (5)) one should compute P_c from Equation (7) in order to be consistent with the PR EoS. For comparison reasons, we will use the P_c from the MC simulations to compute the critical compressibility factor and compare this with the constant PR EoS value of 0.307.

The acentric factor of the gases is obtained from the following definition [2]:

$$\omega = -1.0 - \log(P_r^{sat})_{T_r=0.7} \tag{8}$$

Therefore, ω can be determined from T_c, P_c, and a single reduced vapor pressure ($P_r^{\text{sat}} = P^{\text{sat}}/P_c$) computation at a reduced temperature ($T_r = T/T_c$) of 0.7.

In Table 1, the critical parameters computed for the gases using the three simulation sets are compared with experimental data. The raw data of all the Gibbs ensemble simulations used to fit the parameters can be found in the Supporting Information. For the TraPPE molecules, the results clearly show that the simulations should be performed with a cutoff radius of 14 Å and tail corrections in order to obtain good agreement with experiments. For molecules described by the TraPPE force field, using a 12 Å cutoff radius and without tail corrections has a detrimental effect on the critical temperature,

vapor pressure, and hence the critical pressure. Recently, Dinpajooh *et al.* [38] performed extensive GEMC simulations to investigate the effect of system size, cutoff distance, and tail corrections on the critical properties of LJ particles and n-decane. For these systems, Dinpajooh *et al.* demonstrated that using tail corrections is crucial to obtain accurate results, which is in agreement with our findings for the gases CO_2, CH_4, N_2, and H_2S. The force field parameters of CO were fitted by Martin-Calvo *et al.* [34] using a cutoff of 12 Å and without tail corrections. Therefore, using a cutoff of 14 Å and including tail corrections in the simulations increases the critical temperature and pressure of CO. In Table 1, the critical compressibility factor (Z_C) is also computed from the MC data, which shows that the value of Z_c of the gases is slightly lower than the value of the PR EoS (0.307). Note that the VLE of H_2 extends from 13.95 K to 33.25 K, which cannot be computed from MC simulations using a classical LJ potential, since quantum effects are nonnegligible at these temperatures [41].

3.2. Densities

The densities of the gases have been computed in a temperature range of 300.15-393.15 K and pressures up to 100 bar using MC simulations in the NPT ensemble. This temperature and pressure range is mainly important for natural/synthesis gas production and purification processes. The computed densities will be compared with the reference EoS of the gases implemented in the NIST REFPROP database [42]. The deviation of the densities computed from the MC simulations with respect to the REFPROP data for the gases CH_4, CO, H_2, and N_2 is smaller than 1%, see the Supporting Information. The density difference between the MC simulations and the REFPROP data for the gases CO_2 and H_2S is shown in Figures 1 and 2. For both gases, the MC data deviate significantly from the REFPROP data in regions close to phase transitions and the critical points. Outside these regions, the MC data is in good agreement (i.e., differences are typically smaller than 3%) with the data from REFPROP.

3.3. Fugacities

We recall that the aim is to compute the fugacity of the gases CO_2, CH_4, CO, H_2, N_2, and H_2S from MC simulations and to compare this with the fugacities obtained from the REFPROP database. The fugacity of the gases can be computed directly from MC simulations using Widom's test particle method [43]. However, fugacities computed at high pressures using Widom's

method are typically subjected to large uncertainties [44]. Alternatively, the fugacity of the gases can be computed from PVT data using:

$$\ln \phi = \int_0^p \frac{Z-1}{p} dp \tag{9}$$

where Z is the compressibility factor defined by

$$Z = \frac{PV}{RT}. \tag{10}$$

The molar volume, V, can be computed from MC simulations in the NPT ensemble. For sufficient PVT data, the integral in Equation (9) can be evaluated by the 'graphical method' (i.e., plotting $(Z-1)/p$ vs p and computing the area under the curve) [45]. However, the fugacities are more conveniently computed by fitting the simulation data to an EoS. Here, we use the PR EoS with the critical parameters obtained from the MC simulations to compute the fugacity of the gases. In Table 1, the critical parameters were fitted for different simulation settings. For the TraPPE molecules, the fugacities were computed using the critical parameters from the MC simulations with a 14 Å cutoff and including tail corrections. As mentioned earlier, Martin-Calvo *et al.* [34] fitted the force field parameters of CO for a 12 Å cutoff radius and with tail corrections. Therefore, the critical parameters obtained with these specific simulation settings (i.e., 12 Å cutoff and with tail corrections) were used to compute the fugacity of CO. The EoS approach cannot be used to compute the fugacities of H_2, because the critical parameters of H_2 could not be computed from the MC simulations. For H_2, the 'graphical method' is used to obtain the fugacities. Only the results for CO_2, CH_4, and H_2S will be presented in the main text. Data of the other gases can be found in the Supporting Information. In Figures 3 to 5, the computed fugacity coefficients of CO_2, CH_4, and H_2S are compared with the REFPROP data. Clearly, the deviation increases in the vicinity of the critical points and in the condensed phase. Overall, the deviation in computing the fugacities with the PR EoS using the critical parameters from the MC simulations and the REFPROP database is less than 5%. This in fact implies that the force fields used for the gases in the MC simulations can reproduce the fugacities within 5% of the experimental data.

3.4. Binary systems and binary interaction parameters

The binary interaction parameters (BIPs) used in the PR EoS have an empirical nature and are typically obtained by fitting these to experimental

VLE data [2]. Here, we use MC simulations to compute the VLE of the 15 possible binary systems comprising the gases CO_2, CH_4, CO, H_2, N_2, and H_2S. Subsequently, the binary interaction parameter (k_{ij}) is fitted to the MC data using the PR EoS. The computed BIPs will be compared with the BIPs typically used in process design simulators. A selected number of systems will be presented in the main text and data for the other systems can be found in the Supporting Information. We will emphasize on natural/synthesis gas mixtures and systems that significantly deviate from the experiments. Natural gas typically contains a wide variety of impurities including the sour gases CO_2 and H_2S. Therefore, the sweetening of natural gas requires VLE data on the systems CO_2/CH_4, CO_2/H_2S, and CH_4/H_2S. MC simulatons were used to compute the VLE of CO_2/CH_4 mixtures at a temperature of 270 K. In Figure 6, the MC results are compared with the experimental data of Al-Sahhaf *et al.* [46] and the GERG EoS [32]. The MC simulations slightly overestimate the liquid phase mole fraction of methane, while the gas phase is accurately described. The VLE of the system CO_2/H_2S is computed at 273.15 K and a comparison with the experimental data of Chapoy *et al.* [47] is presented in Figure 7. The MC data is in good agreement with the experiments and the GERG EoS results. The VLE of the system CH_4/H_2S has been computed at 313.08 K and a comparison of the MC data with the experiments of Coquelet *et al.* [48] is presented in Figure 8. Clearly, the MC simulations overestimate the solubility of methane in the liquid phase, but the gas phase composition is correctly predicted. Our MC results for the CH_4/H_2S mixture are in good agreement with the MC simulations of Shah *et al.* [33], although these authors used the explicit-hydrogen version of the TraPPE force field for methane.

Synthesis gas or syngas typically contains a mixture of CO_2, CO, and H_2. Hence, it is important to consider the VLE of the binary systems CO_2/CO, CO_2/H_2, and CO/H_2. We have computed the VLE of the CO_2/CO system at 253.15 K and a comparison with experimental data of Kaminishi *et al.* [49] is presented in Figure 9. The MC simulations slightly overestimate (underestimate) the CO mole fraction in the gas phase (liquid phase). Moreover, the GERG EoS is not able to correctly describe the VLE of this mixture, whereas the PR EoS with a k_{ij} of -0.05 correctly captures the VLE. In Figure 10, the computed VLE of CO_2/H_2 is compared with the experimental data of Fandino *et al.* [50] at a temperature of 258.15 K. The MC simulations correctly predicts the liquid phase mole fractions of H_2, but overestimate the H_2 molefractions in the gas phase. In Figure 11, the MC results for the sys-

tem CO/H_2 is compared with the experimental data of Akers and Eubanks [51] at 99.82 K. The MC simulations significantly overpredict the solubility of H_2 in the liquid phase and slightly overpredict the mole fractions of H_2 in the gas phase. For this system, the GERG EoS failed to converge, but the PR EoS with a k_{ij} of 0.0544 correctly predicts the VLE of CO/H_2 mixtures.

The MC data of the systems CH_4/H_2, H_2S/N_2, and H_2S/CO deviate significantly from the experimental data, see Figures 12 to 14. For all the three systems, the solubility of the diatomic gas in the liquid phase is overestimated, while the composition of the gas phase is correctly predicted. Experimental VLE data for the system H_2S/H_2 have not been reported so far. However, we have estimated the coexisting conditions of this binary system from the H_2S/N_2 system and computed the VLE of H_2S/H_2 mixtures using MC simulations, see Supporting Information. The accuracy of the MC simulations for this system cannot be verified, hence the data should be treated with caution.

Subsequently, the binary interaction parameters (k_{ij}) of the PR EoS were fitted to the VLE data from the MC simulations. In Table 2, the BIPs used in the procces simulator Aspen Plus [52] have been reported. The corresponding BIPs computed from the MC data are reported in Table 3. The BIPs computed from the simulations deviate significantly from the BIPs used in Aspen Plus for the systems CO_2/CO, CO_2/H_2, CH_4/CO, CH_4/H_2, CO/N_2, CO/H_2S, H_2/H_2S, and N_2/H_2S. The BIPs were fitted to the bubble-point curves, but for these systems the bubble points computed from the MC simulations deviated (slightly) from the experimental bubble-point curves. For the other systems, the computed BIPs are in agreement with BIPs used in Aspen Plus. Note that BIPs are typically temperature dependent [53–55], but Aspen Plus uses a temperature independent BIP for the investigated gas mixtures, which complicates a direct comparison with our results.

3.5. Ternary systems

In addition to the binary systems, we have computed the ternary phase diagram of the systems $CO_2/H_2S/CH_4$ and $CO_2/CO/H_2$ relevant for natural gas sweetening and the precombustion process, respectively. The VLE of the ternary $CO_2/H_2S/CH_4$ mixture is computed at a temperature of 277.6 K and at a pressure of 2.76 MPa. In Figure 15, the MC results are compared with the experimental data of Besserer and Robinson [56]. The MC data is in good

agreement with the experiments, but the gas phase mole fractions of methane is slightly overestimated. Recently, Shah *et al.* [33] computed the VLE of the $CO_2/H_2S/CH_4$ system at 238.8 K and 3.45 MPa using MC simulations. Shah *et al.* used the explicit-hydrogen model of CH_4, whereas the united-atom model of CH_4 is used here. These authors also found that the methane mole fractions in the gas phase was overestimated. The VLE of the ternary $CO_2/CO/H_2$ mixture is computed at 253.15 K and 10.1 MPa. In Figure 16, the MC results are compared with the experimental data of Kaminishi et al. [49]. Overall, the MC results are in good agreement with the experiments, but the CO mole fractions in the gas phase is slightly overestimated. This is expected, since the CO mole fraction in the gas phase was also overestimated in the binary CO_2/CO system, see Figure 9.

4. Conclusion

Molecular simulation is an alternative to the more widely used equation of state (EoS) approach to compute phase equilibria of complex systems. In order to reduce simulation time, MC simulations in ensembles with a fixed chemical potential or fugacity often make use of an EoS to describe the gas phase. However, the fugacities can also be computed from molecular simulations using an accurate force field for the gas molecules. Here, we investigated the consistency of both approaches to compute fugacities of the industrially relevant gases CO_2, CH_4, CO, H_2, N_2, and H_2S. The critical temperatures (T_c), critical presssures (P_c), acentric factors (ω), densities (ρ), and fugacities (f) of the gases CO_2, CH_4, CO, H_2, N_2, and H_2S were computed using MC simulations in the Gibbs ensemble and the NPT ensemble. The effect of cut-off radius and tail corrections on these properties was investigated. For the TraPPE force field, it is crucial to use a cutoff of 14Å and tail corrections in the simulations. The critical properties computed from the MC simulations using the correct force field specifications are in good agreement with experimental data. Close to critical points and phase transitions, the densities of all the gases computed from the MC simulations deviate significantly (up to 10%) from the experimental data, but outside these regions good agreement with the experiments is observed. The MC results show that the used force fields of the gases can reproduce the fugacities within 5% of the experimental data. MC simulations in the Gibbs ensemble was used to compute the 15 binary systems comprising the gases CO_2, CH_4, CO, H_2, N_2, and H_2S, and the ternary systems $CO_2/H_2S/CH_4$ and $CO_2/CO/H_2$. The dew-point curves

of all the 15 binaries were predicted correctly by the MC simulations, but the bubble-point curves for the systems H_2/CO, CH_4/H_2, H_2S/N_2, and H_2S/CO deviate significantly from the experiments. For the system CO_2/CO, the GERG EoS highly underestimate the gas and liquid phase composition of CO, while the MC data is in good agreement with the experiments. The binary interaction parameters of the PR EoS were fitted to the VLE data of the 15 binary systems computed from the MC simulations. These binary interaction parameters are important to describe the adsorption/absorption behavior of gas mixtures in adsorbents/solvents. The binary interaction parameters computed from the MC data for mixtures containing CO, N_2, or H_2, deviate significantly from the binary interaction parameters used in Aspen Plus. The VLE of the ternary systems CO_2/H_2S/CH_4 and CO_2/CO/H_2 computed from the MC simulations are in good agreement with experiments.

Acknowledgments

We thank Prof. Theo de Loos for his mentorship and the many stimulating scientific discussions we had over the past years. This work was sponsored by NWO Exacte Wetenschappen (Physical Sciences) for the use of supercomputer facilities, with financial support from the Nederlandse Organisatie voor Wetenschappelijk Onderzoek (Netherlands Organization for Scientific Research, NWO).

Supporting Information

Force field parameters of all the studied components, density data, VLE data of the unary, binary, and ternary systems can be found here.

Table 1: Critical density (ρ_c), temperature (T_c), pressure (P_c), compressibility (Z_c) and acentric factor (ω) of the gases from experiments and MC simulations.

Component	ρ_c / kg/m^3	T_c / K	P_c / MPa	Z_c	ω
Experimental data [57]					
CO_2	467.6	304.1	7.374	0.274	0.225
CH_4	162.6	190.6	4.599	0.286	0.012
CO	303.9	132.9	3.494	0.292	0.045
H_2	31.0	33.3	1.297	0.305	-0.216
N_2	313.3	126.2	3.398	0.290	0.037
H_2S	347.3	373.4	8.963	0.283	0.090
MC data, 12 Å, no tail corrections					
CO_2	467.8	295.2	7.60	0.291	0.249
CH_4	162.5	176.2	4.09	0.276	-0.012
CO	305.3	134.8	3.43	0.281	0.027
N_2	309.4	119.2	3.16	0.289	0.037
H_2S	347.0	356.6	8.55	0.284	0.097
MC data, 14 Å, no tail corrections					
CO_2	465.6	298.9	7.53	0.286	0.240
CH_4	160.2	182.7	4.44	0.293	-0.015
CO	304.9	138.2	3.46	0.276	-0.006
N_2	306.8	122.1	3.21	0.289	0.021
H_2S	346.1	362.2	8.49	0.278	0.083
MC data, 14 Å, with tail corrections					
CO_2	465.4	303.1	7.57	0.284	0.218
CH_4	159.6	187.4	4.54	0.293	-0.017
CO	304.6	140.7	3.74	0.294	0.04
N_2	305.8	124.5	3.29	0.291	0.022
H_2S	348.2	369.4	8.88	0.283	0.089

Table 2: Binary interaction parameters (k_{ij}) of gas mixtures used in Aspen Plus for the PR EoS.

gas pair	CO_2	CH_4	CO	H_2	N_2	H_2S
CO_2	x	0.0919	-0.05[a]	-0.1622	-0.017	0.0974
CH_4	x	x	0.03	0.0156	0.0311	0.0503[b]
CO	x	x	x	0.0544	0.0307	0.0544
H_2	x	x	x	x	0.103	N/A[c]
N_2	x	x	x	x	x	0.1767
H_2S	x	x	x	x	x	x

[a] Fitted to VLE data of Kaminishi *et al.* [49]. [b] Taken from Hajipour *et al.* [58]. [c] Not available.

Table 3: Binary interaction parameters (k_{ij}) of the gas mixtures computed from MC data. MC simulations were performed with a cutoff radius of 14 Å and with tail corrections.

gas pair	CO_2	CH_4	CO	H_2	N_2	H_2S
CO_2	x	0.06	0.01	0.09	-0.07	0.09
CH_4	x	x	-0.04	-0.16	-0.01	0.02
CO	x	x	x	0.01	-0.02	-0.10
H_2	x	x	x	x	0.14	-0.08
N_2	x	x	x	x	x	-0.07
H_2S	x	x	x	x	x	x

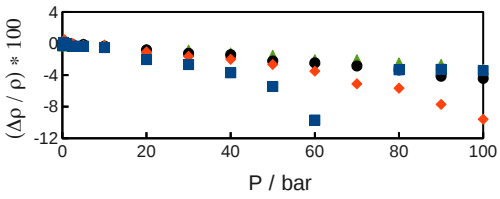

Figure 1: The difference between the densities of CO_2 computed from the MC simulations with respect to the REFPROP data at 300.15 K (squares), 333.15 K (diamonds), 363.15 K (circles), and 393.15 K (triangles). MC simulations were performed with a cutoff radius of 14 Å and tail corrections.

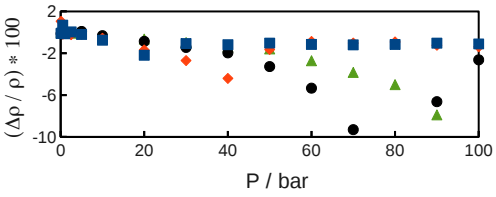

Figure 2: The difference between the densities of H_2S computed from the MC simulations with respect to the REFPROP data at 300.15 K (squares), 333.15 K (diamonds), 363.15 K (circles), and 393.15 K (triangles). MC simulations were performed with a cutoff radius of 14 Å and tail corrections.

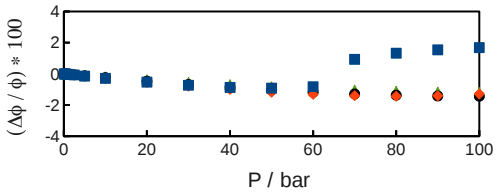

Figure 3: The difference between the fugacity coefficient of CO_2 computed from the MC simulations with respect to the REFPROP data at 300.15 K (squares), 333.15 K (diamonds), 363.15 K (circles), and 393.15 K (triangles). MC simulations were performed with a cutoff radius of 14 Å and tail corrections.

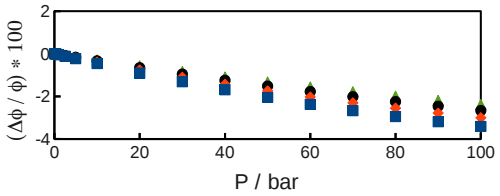

Figure 4: The difference between the fugacity coefficient of CH_4 computed from the MC simulations with respect to the REFPROP data at 300.15 K (squares), 333.15 K (diamonds), 363.15 K (circles), and 393.15 K (triangles). MC simulations were performed with a cutoff radius of 14 Å and tail corrections.

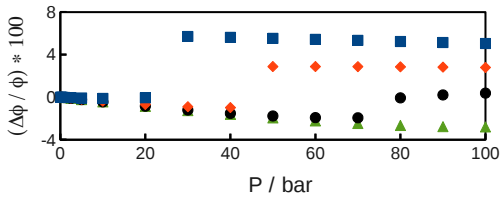

Figure 5: The difference between the fugacity coefficient of H_2S computed from the MC simulations with respect to the REFPROP data at 300.15 K (squares), 333.15 K (diamonds), 363.15 K (circles), and 393.15 K (triangles). MC simulations were performed with a cutoff radius of 14 Å and tail corrections.

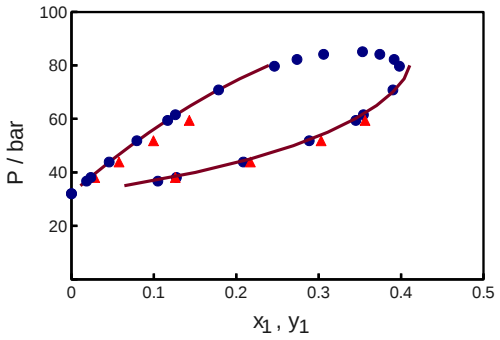

Figure 6: VLE of the binary system CH_4 (1) + CO_2 (2) at 270 K. Experimental data (circles) from Al-Sahhaf *et al.* [46], MC data (triangles), and GERG EoS modeling results (lines). MC simulations were performed with a cutoff radius of 14 Å and tail corrections.

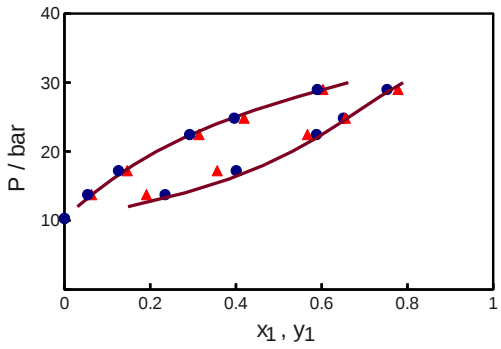

Figure 7: VLE of the binary system CO_2 (1) + H_2S (2) at 273.15 K. Experimental data (circles) from Chapoy *et al.* [47], MC data (triangles), and GERG EoS modeling results (lines). MC simulations were performed with a cutoff radius of 14 Å and tail corrections.

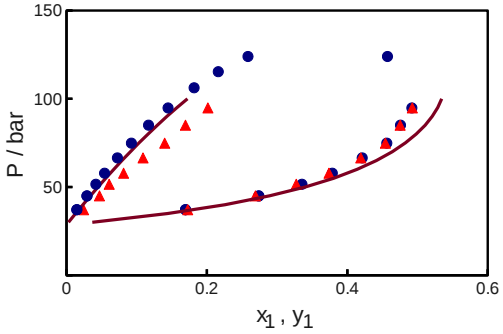

Figure 8: VLE of the binary system CH_4 (1) + H_2S (2) at 313.08 K. Experimental data (circles) from Coquelet *et al.* [], MC data (triangles), and GERG EoS modeling results (lines). MC simulations were performed with a cutoff radius of 14 Å and tail corrections.

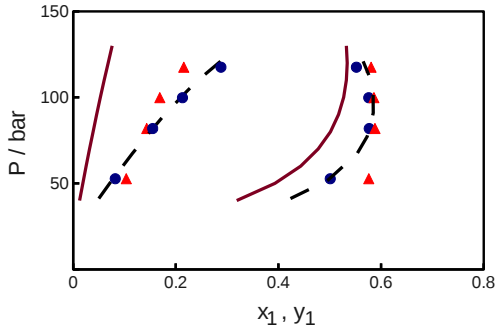

Figure 9: VLE of the binary system CO (1) + CO_2 (2) at 253.15 K. Experimental data (circles) from Kaminishi *et al.* [49], MC data (triangles), GERG EoS modeling results (solid lines), and PR EoS modeling with a k_{ij} of -0.05 (dashed lines). MC simulations were performed with a cutoff radius of 14 Å and tail corrections.

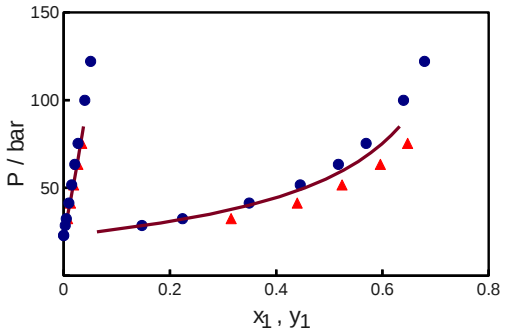

Figure 10: VLE of the binary system H_2 (1) + CO_2 (2) at 258.15 K. Experimental data (circles) from Fandino *et al.* [50], MC data (triangles), and GERG EoS modeling results (lines). MC simulations were performed with a cutoff radius of 14 Å and tail corrections.

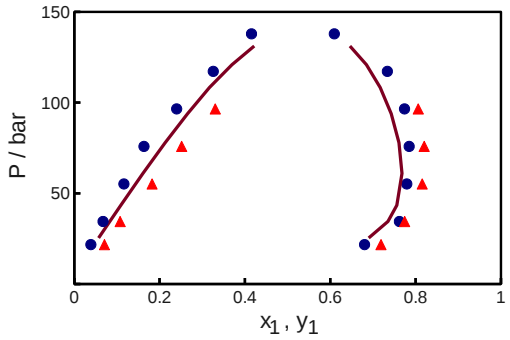

Figure 11: VLE of the binary system H_2 (1) + CO (2) at 99.82 K. Experimental data (circles) from Akers and Eubanks [51], MC data (triangles), and PR EoS modeling with a k_{ij} of 0.0544 (lines). The GERG EoS failed to converge for this system. MC simulations were performed with a cutoff radius of 14 Å and tail corrections.

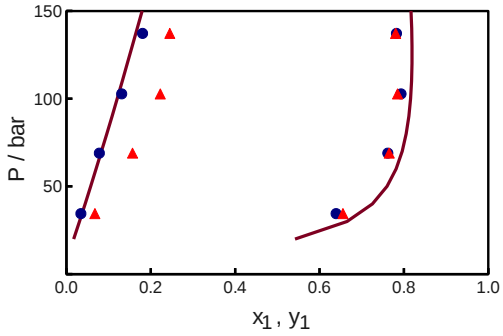

Figure 12: VLE of the binary system H_2 (1) + CH_4 (2) at 144.26 K. Experimental data (circles) from Benham and Katz [59], MC data (triangles), and GERG EoS modeling (lines). MC simulations were performed with a cutoff radius of 14 Å and tail corrections.

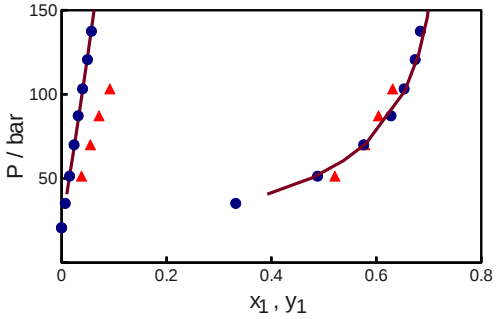

Figure 13: VLE of the binary system N_2 (1) + H_2S (2) at 300.04 K. Experimental data (circles) from Besserer and Robinson [56], MC data (triangles), and GERG EoS modeling (lines). MC simulations were performed with a cutoff radius of 14 Å and tail corrections.

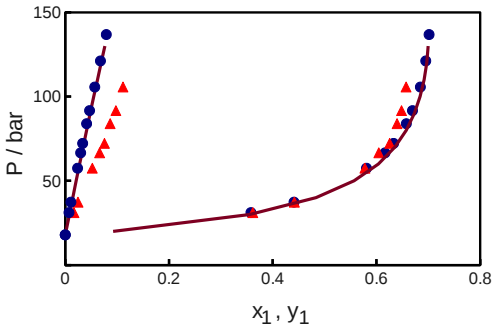

Figure 14: VLE of the binary system CO (1) + H_2S (2) at 293.15 K. Experimental data (circles) from Fredenslund and Mollerup [60], MC data (triangles), and GERG EoS modeling (lines). MC simulations were performed with a cutoff radius of 14 Å and tail corrections.

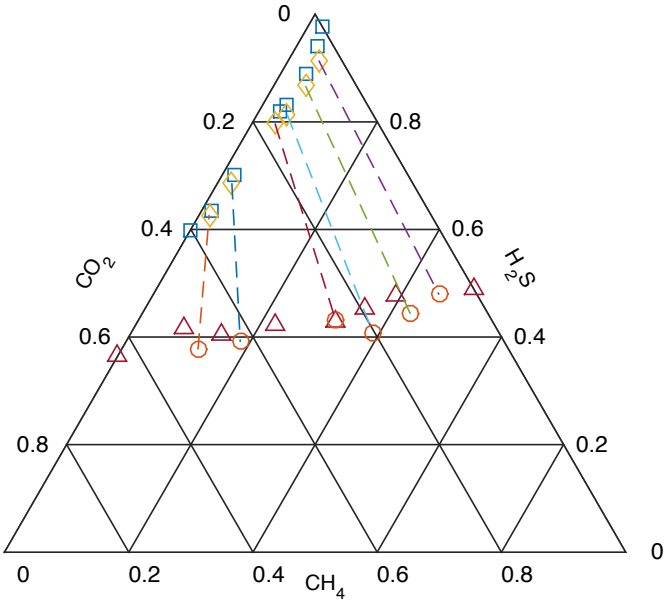

Figure 15: VLE of the ternary system $CO_2/H_2S/CH_4$ at 277.6 K and 2.76 MPa. Experimental liquid phase (squares) and gas phase (triangles) composition from Robinson *et al.* [61], and MC data of the liquid phase (diamonds) and gas phase composition (circles). MC simulations were performed with a cutoff radius of 14 Å and tail corrections.

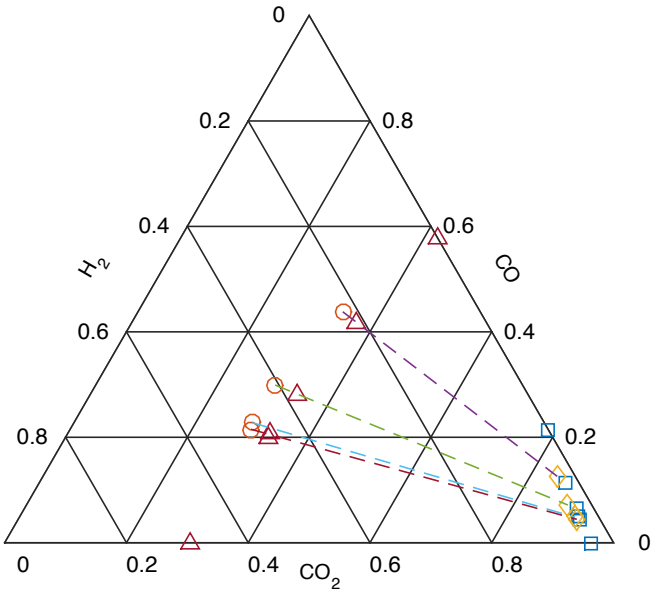

Figure 16: VLE of the ternary system $CO_2/CO/H_2$ at 253.15 K and 10.1 MPa. Experimental liquid phase (squares) and gas phase (triangles) composition from Kaminishi *et al.* [49], and MC data of the liquid phase (diamonds) and gas phase composition (circles). MC simulations were performed with a cutoff radius of 14 Å and tail corrections.

References

[1] J. D. Seader, E. J. Henley, D. K. Roper, Separation Process Principles, 3rd Edition, Wiley, New York, 2013.

[2] J. M. Smith, H. C. V. Ness, M. M. Abbott, Introduction to Chemical Engineering Thermodynamics, 7th Edition, Mc Graw Hill, New York, 2005.

[3] J. M. Prausnitz, R. N. Lichtenthaler, E. Gomes de Azevedo, Molecular Thermodynamics of Fluid-Phase Equilibria, 3rd Edition, Prentice Hall PTR, New Jersey, USA, 1999.

[4] D. Frenkel, B. Smit, Understanding Molecular Simulation: From Algorithms to Applications, 2nd Edition, Academic Press, San Diego, USA, 2002.

[5] M. P. Allen, D. J. Tildesley, Computer Simulation of Liquids, Oxford University Press, New York, USA, 1987.

[6] J. J. de Pablo, Q. Yan, F. A. Escobedo, Simulation of Phase Transitions in Fluids, Annu. Rev. Phys. Chem. 50 (1999) 377–411.

[7] F. A. Escobedo, Novel pseudoensembles for simulation of multicomponent phase equilibria, J. Chem. Phys. 108 (1998) 8761–8772.

[8] A. Z. Panagiotopoulos, Monte Carlo methods for phase equilibria of fluids, J. Phys.: Condens. Matter 12 (2000) R25–R52.

[9] Q. Chen, S. P. Balaji, M. Ramdin, J. J. Gutiérrez-Sevillano, A. Bardow, E. Goetheer, T. J. H. Vlugt, Validation of the CO_2/N_2O Analogy Using Molecular Simulation, Ind. Eng. Chem. Res. 53 (2014) 18081–18090.

[10] M. Ramdin, S. P. Balaji, J. M. Vicent-Luna, J. J. Gutiérrez-Sevillano, S. Calero, T. W. de Loos, T. J. H. Vlugt, Solubility of the Precombustion Gases CO_2, CH_4, CO, H_2, N_2, and H_2S in the Ionic Liquid [bmim][Tf_2N] from Monte Carlo Simulations, J. Phys. Chem. C 118 (2014) 23599–23604.

[11] M. Ramdin, Q. Chen, S. P. Balaji, J. M. Vicent-Luna, A. Torres-Knoop, D. Dubbeldam, S. Calero, T. W. de Loos, T. J. H. Vlugt, Solubilities of

CO_2, CH_4, C_2H_6, and SO_2 in ionic liquids and Selexol from Monte Carlo simulations, J. Comput. Sci. (in press). doi:10.1016/j.jocs.2015.09.002.

[12] S. P. Balaji, S. Gangarapu, M. Ramdin, A. Torres-Knoop, H. Zuilhof, E. L. V. Goetheer, D. Dubbeldam, T. J. H. Vlugt, Simulating the Reactions of CO_2 in Aqueous Monoethanolamine Solution by Reaction Ensemble Monte Carlo Using the Continuous Fractional Component Method, J. Chem. Theory Comput. 11 (2015) 2661–2669.

[13] M. Ramdin, S. P. Balaji, J. M. Vicent-Luna, A. Torres-Knoop, D. Dubbeldam, S. Calero, T. W. de Loos, T. J. H. Vlugt, Computing bubble-points of CO_2/CH_4 gas mixtures in ionic liquids from Monte Carlo simulations, Fluid Phase Equilib. (in press). doi:10.1016/j.fluid.2015.09.041.

[14] M. Ramdin, S. P. Balaji, A. Torres-Knoop, D. Dubbeldam, T. W. de Loos, T. J. H. Vlugt, Solubility of Natural Gas Species in Ionic liquids and Commercial Solvents: Experiments and Monte Carlo Simulations, J. Chem. Eng. Data 60 (2015) 3039–3045.

[15] S. Budhathoki, J. K. Shah, E. J. Maginn, Molecular Simulation Study of the Solubility, Diffusivity and Permselectivity of Pure and Binary Mixtures of CO_2 and CH_4 in the Ionic Liquid 1-n-Butyl-3-methylimidazolium bis(trifluoromethylsulfonyl)imide, Ind. Eng. Chem. Res. 54 (2015) 8821–8828.

[16] E. J. Maginn, Molecular simulation of ionic liquids: current status and future opportunities, J. Phys.: Condens. Matter 21 (2009) 1–17.

[17] E. J. Maginn, Atomistic Simulation of the Thermodynamic and Transport Properties of Ionic Liquids, Acc. Chem. Res. 40 (2007) 1200–1207.

[18] W. Shi, E. J. Maginn, Molecular Simulation and Regular Solution Theory Modeling of Pure and Mixed Gas Absorption in the Ionic Liquid 1-n-Hexyl-3-methylimidazolium Bis(Trifluoromethylsulfonyl)amide ([hmim][Tf_2N]), J. Phys. Chem. B 112 (2008) 16710–1670.

[19] W. Shi, E. J. Maginn, Atomistic Simulation of the Absorption of Carbon Dioxide and Water in the Ionic Liquid 1-n-Hexyl-3-methylimidazolium Bis(trifluoromethylsulfonyl)imide ([hmim][Tf_2N]), J. Phys. Chem. B 112 (2008) 2045–2055.

[20] W. Shi, E. J. Maginn, Improvement in Molecule Exchange Efficiency in Gibbs Ensemble Monte Carlo: Development and Implementation of the Continuous Fractional Component Move, J. Comput. Chem. 29 (2008) 2520–2530.

[21] D. Dubbeldam, A. Torres-Knoop, K. S. Walton, On the inner workings of Monte Carlo codes, Mol. Simul. 39 (2013) 1253–1392.

[22] D. Dubbeldam, S. Calero, D. E. Ellis, R. Q. Snurr, RASPA: molecular simulation software for adsorption and diffusion in flexible nanoporous materials, Mol. Simul. 42 (2016) 81–101.

[23] J. O. Valderrama, The State of the Cubic Equations of State, Ind. Eng. Chem. Res. 42 (2003) 1603–1618.

[24] Y. S. Wei, R. J. Sadus, Equations of State for the Calculation of Fluid-Phase Equilibria, AIChE J. 46 (2000) 169–196.

[25] G. Kontogeorgis, G. Folas, Thermodynamic Models for Industrial Applications: From Classical and Advanced Mixing Rules to Association Theories, Wiley, Chichester, UK, 2010.

[26] D. Browarzik, J. P. M. Trusler, I. G. Economou, J. Ely, C. McCabe, A. Galindo, M. A. Anisimov, M. C. Kroon, E. Lemmon, S. Bottini, E. Brignole, S. Pereda, S. Kjelstrup, D. Bedeaux, S. I. Sandler, Applied Thermodynamics of Fluids, The Royal Society of Chemistry, 2011.

[27] H. Orbey, S. I. Sandler, Modeling Vapor-Liquid Equilibria: Cubic Equations of State and Their Mixing Rules, no. v. 1 in Cambridge Series in Chemical Engineering, Cambridge University Press, 1998.

[28] J. J. Potoff, J. I. Siepmann, Vapor-Liquid Equilibria of Mixtures Containing Alkanes, Carbon Dioxide, and Nitrogen, AIChE J. 47 (2001) 1676–1682.

[29] M. G. Martin, J. I. Siepmann, Transferable potentials for phase equilibria. 1. United-atom description of n-alkanes, J. Phys. Chem. B 102 (1998) 2569–2577.

[30] J. Gross, G. Sadowski, Perturbed-chain saft: An equation of state based on a perturbation theory for chain molecules, Ind. Eng. Chem. Res. 40 (4) (2001) 1244–1260.

[31] D. Peng, D. B. Robinson, A New Two-Constant Equation of State, Ind. Eng. Chem. Fundam. 15 (1976) 59–64.

[32] O. Kunz, W. Wagner, The GERG-2008 Wide-Range Equation of State for Natural Gases and Other Mixtures: An Expansion of GERG-2004, J. Chem. Eng. Data 57 (2012) 3032–3091.

[33] M. S. Shah, M. Tsapatsis, J. I. Siepmann, Development of the Transferable Potentials for Phase Equilibria Model for Hydrogen Sulfide, J. Phys. Chem. B 119 (2015) 7041–7052.

[34] A. Martín-Calvo, F. D. Lahoz-Martín, S. Calero, Understanding Carbon Monoxide Capture Using Metal-Organic Frameworks, J. Phys. Chem. C 116 (2012) 6655–6663.

[35] R. F. Cracknell, Molecular simulation of hydrogen adsorption in graphitic nanofibres, Phys. Chem. Chem. Phys. 3 (2001) 2091–2097.

[36] P. P. Ewald, Die Berechnung optischer und elektrostatischer gitterpotentiale, Ann. Phys. 64 (1921) 253–287.

[37] R. D. Weir, T. W. de Loos, Measurement of the Thermodynamic Properties of Multiple Phases, Elsevier, 2005.

[38] M. Dinpajooh, P. Bai, D. A. Allan, J. I. Siepmann, Accurate and precise determination of critical properties from Gibbs ensemble Monte Carlo simulations, J. Chem. Phys. 143 (2015) 114113.

[39] E. Kiran, J. Sengers, Supercritical Fluids: Fundamentals for Application, Nato Science Series E: Applied Sciences, Springer Netherlands, 1994.

[40] A. M. Abudour, S. A. Mohammad, R. L. Robinson Jr., K. A. M. Gasem, Generalized binary interaction parameters for the Peng-Robinson equation of state, Fluid Phase Equilib. 383 (2014) 156–173.

[41] O. Kunz, W. Wagner, The GERG-2008 Wide-Range Equation of State for Natural Gases and Other Mixtures: An Expansion of GERG-2004, J. Phys. Chem. C 117 (2013) 14374–14380.

[42] E. W. Lemmon, M. L. Huber, M. O. McLinden, NIST Standard Reference Database 23 (2013).

[43] B. Widom, Statistical Mechanics: A concise introduction for chemists, Cambridge University Press, Cambridge, UK, 2002.

[44] J. Vrabec, M. Kettler, H. Hasse, Chemical potential of quadrupolar two-centre lennard-jones fluids by gradual insertion, Chem. Phys. Lett. 356 (56) (2002) 431 – 436.

[45] S. Walas, Phase Equilibria in Chemical Engineering, Elsevier Science, 2013.

[46] T. A. Al-Sahhaf, A. J. Kidnay, E. D. Sloan, Liquid + Vapor Equilibria in the N_2 + CO_2 + CH_4 System, Ind. Eng. Chem. Fundam. 22 (1983) 372–380.

[47] A. Chapoy, C. Coquelet, H. Liu, A. Valtz, B. Tohidi, Vapour-liquid equilibrium data for the hydrogen sulphide (H_2S) + carbon dioxide (CO_2) system at temperatures from 258 to 313 K, Fluid Phase Equilib. 356 (2013) 223–228.

[48] C. Coquelet, A. Valtz, P. Stringari, M. Popovic, D. Richon, P. Mougin, Phase equilibrium data for the hydrogen sulphide + methane system at temperatures from 186 to 313 K and pressures up to about 14 MPa, Fluid Phase Equilib. 383 (2014) 94–99.

[49] G. Kaminishi, Y. Arai, S. Saito, S. Maeda, Vapor-liquid equilibria for the binary and ternary systems containing carbon dioxide, J. Chem. Eng. Jpn. 1 (1968) 109–116.

[50] O. Fandino, J. P. M. Trusler, D. Vega-Maza, Phase behavior of (CO_2 + H_2) and (CO_2 + N_2) at temperatures between (218.15 and 303.15) K at pressures up to 15 MPa, Int. J. Greenh. Gas Cont. 36 (2015) 78–92.

[51] W. W. Akers, L. S. Eubanks, Advances in Cryogenic Engineering: Proceedings of the 1957 Cryogenic Engineering Conference, National Bureau of Standards Boulder, Colorado, August 19–21, 1957, Springer US, Boston, MA, 1960, Ch. Vapor-Liquid Equilibria in the System Hydrogen-Nitrogen-Carbon Monoxide, pp. 275–293.

[52] Aspen Technology, Inc., Aspen properties reference manual, Aspen Technology, Inc., Burlington, MA, USA, 2006.

[53] R. Privat, J. Jaubert, CO_2 Sequestration and Valorization, INTECH, 2014, Ch. Predicting the Phase Equilibria of Carbon Dioxide Containing Mixtures Involved in CCS Processes Using the PPR78 Model, pp. 443–462.

[54] J. Jaubert, F. Mutelet, VLE predictions with the Peng-Robinson equation of state and temperature dependent kij calculated through a group contribution method, Fluid Phase Equilibria 224 (2004) 285–304.

[55] J. M. Moysan, H. Paradowski, J. Vidal, Prediction of phase behaviour of Gas-containing systems with cubic equations of state, Chem. Eng. Sci. 41 (1986) 2069–2074.

[56] G. J. Besserer, D. B. Robinson, Equilibrium-Phase Properties of Nitrogen-Hydrogen Sulfide System, J. Chem. Eng. Data 20 (1975) 157–161.

[57] B. E. Poling, J. M. Prausnitz, J. P. O'Connell, The Properties of Gases and Liquids, 5th Edition, Mc Graw Hill, Singapore, 2007.

[58] S. Hajipour, M. A. Satyro, M. W. Foley, Uncertainty analysis applied to thermodynamic models and process design-2. Binary mixtures, Fluid Phase Equilibria 364 (2014) 15–30.

[59] A. L. Benham, D. L. Katz, Vapor-liquid Equilibria for Hydrogen-light-Hydrocarbon Systems at Low Temperatures, AIChE J. 3 (1957) 33–36.

[60] A. Fredenslund, J. Mollerup, Gas-liquid equilibrium of hydrogen sulphide + carbon monoxide, J. Chem. Thermodyn. 7 (1975) 677–682.

[61] D. B. Robinson, A. P. Lorenzo, C. A. A. Macrygeorgos, The Carbon Dioxide-Hydrogen Sulphide-Methane System: Part II. Phase Behavior at 40 °F. and 160 °F., Can. J. Chem. Eng. December (1959) 212–217.